

REPLAY: Modeling Time-Varying Temporal Regularities of Human Mobility for Location Prediction over Sparse Trajectories

Bangchao Deng¹, Bingqing Qu², Pengyang Wang¹ and Dingqi Yang^{*1}

¹University of Macau

²BNU-HKBU United International College

yc37980@um.edu.mo, bingqingqu@uic.edu.cn, {pywang,dingqiyang}@um.edu.mo

Abstract

Location prediction forecasts a user’s location based on historical user mobility traces. To tackle the intrinsic sparsity issue of real-world user mobility traces, spatiotemporal contexts have been shown as significantly useful. Existing solutions mostly incorporate spatiotemporal distances between locations in mobility traces, either by feeding them as additional inputs to Recurrent Neural Networks (RNNs) or by using them to search for informative past hidden states for prediction. However, such distance-based methods fail to capture the time-varying temporal regularities of human mobility, where human mobility is often more regular in the morning than in other periods, for example; this suggests the usefulness of the actual timestamps besides the temporal distances. Against this background, we propose REPLAY, a general RNN architecture learning to capture the time-varying temporal regularities for location prediction. Specifically, REPLAY not only resorts to the spatiotemporal distances in sparse trajectories to search for the informative past hidden states, but also accommodates the time-varying temporal regularities by incorporating smoothed timestamp embeddings using Gaussian weighted averaging with timestamp-specific learnable bandwidths, which can flexibly adapt to the temporal regularities of different strengths across different timestamps. Our extensive evaluation compares REPLAY against a sizable collection of state-of-the-art techniques on two real-world datasets. Results show that REPLAY consistently and significantly outperforms state-of-the-art methods by 7.7%-10.9% in the location prediction task, and the bandwidths reveal interesting patterns of the time-varying temporal regularities.

1 Introduction

Location prediction is a key problem in human mobility modeling, serving as a fundamental building block for various location based services. The primary task is to predict a

user’s future location based on the user’s historical mobility traces [Noulas *et al.*, 2012b]. As a sequence modeling problem by nature, location prediction problems have been widely tackled by the literature using Recurrent Neural Networks (RNNs), such as vanilla RNN [Mikolov *et al.*, 2010], Long Short-Term Memory (LSTM) [Hochreiter and Schmidhuber, 1997] and Gated Recurrent Unit (GRU) [Cho *et al.*, 2014]; these techniques have shown great success in language modeling to learn from word sequences. However, different from word sequences (i.e., text sentences), real-world user mobility traces are often *sparse and incomplete*, due to the nature of the data collection scheme and privacy issues. More precisely, on Location Based Social Networks (LBSNs) which are widely used as a primary data source for benchmarking location prediction techniques, users voluntarily share their spatiotemporal presence (check-ins) at a specific Point of Interest (POI) at a specific time; such a *voluntary* sharing protocol intrinsically implies sparse mobility traces. For example, an empirical study on a widely used Foursquare dataset shows that the median time between successive check-ins is about 16.72 hours [Deng *et al.*, 2023]. Such sparsity and incompleteness hinder the application of RNNs to the location prediction problem.

To tackle this sparsity issue, existing works strive to extend RNN architectures by incorporating spatiotemporal contexts, which have been shown as strong predictors for location prediction [Gonzalez *et al.*, 2008]. A widely adopted approach is to add the spatiotemporal distances between successive check-ins as additional inputs together with sequences of POIs to RNN units [Liu *et al.*, 2016; Neil *et al.*, 2016; Zhu *et al.*, 2017; Kong and Wu, 2018; Cui *et al.*, 2019; Zhao *et al.*, 2019; Zhao *et al.*, 2020]. Despite its wide adoption, recent studies have shown that this approach cannot fully capture the temporal periodicity and spatial regularity of human mobility patterns [Yang *et al.*, 2020a], as considering spatiotemporal distances between check-ins that are several steps apart (i.e., high-order distances) in the check-in sequences are often more informative than those between successive check-ins for location prediction. Subsequently, a flashback mechanism has been introduced to explicitly use such high-order spatiotemporal distances to search past hidden states with high predictive power (i.e., historical hidden states with similar spatiotemporal contexts to the current one) [Yang *et al.*, 2020a; Li *et al.*, 2021a; Cao *et al.*, 2021;

*Corresponding author

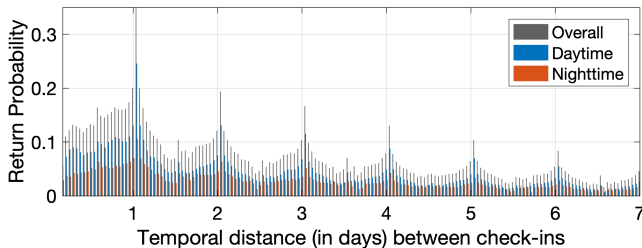


Figure 1: Returning probability w.r.t. the temporal distances between check-ins. We plot the overall returning probability and its breakdown in the daytime (6:00-18:00) or nighttime (18:00-6:00). We observe that the daytime returning probability is significantly higher than in nighttime, which implies that the temporal regularity is much stronger in the daytime than in the nighttime.

Rao *et al.*, 2022; Liu *et al.*, 2022; Wu *et al.*, 2022; Ye *et al.*, 2023]. However, despite the improved performance, the temporal distances still fail to capture the time-varying temporal regularities of human mobility, as we discuss below.

Temporal regularity has been revealed as a universal law of human mobility [Gonzalez *et al.*, 2008; Noulas *et al.*, 2012a], which can be evidenced by the periodicity of human activities even in sparse human mobility traces [Cho *et al.*, 2011]. Figure 1 illustrates the returning probability of user check-ins over time on the Foursquare dataset, which is defined as the probability of a user re-checking in at a POI a certain period of time after her first check-in at that POI [Gonzalez *et al.*, 2008; Lian *et al.*, 2015]. We observe an obvious daily (periodic) revisiting pattern, which implies that the historical check-ins with a temporal distance closer to these daily peaks have higher predictive power; this serves as the foundation for the flashback mechanism [Yang *et al.*, 2020a]. In this paper, we further reveal that *the strength of the temporal regularities varies across different time periods during a day (or across different days in a week, e.g., weekdays v.s. weekends)*. On the Foursquare dataset, the mobility pattern in the daytime is mostly attributed to working-related activities, which is usually more regular than the nighttime mobility pattern that is mostly attributed to entertainment-related activities¹. Figure 1 also compares the daytime and nighttime returning probabilities, where the daytime returning probability is significantly higher than nighttime, implying that the temporal regularity is much stronger in the daytime than in the nighttime. This implies that the hidden state 24 hours back is more informative for location prediction if the current time is daytime rather than nighttime. However, such time-varying temporal regularities cannot be captured by the distance-based methods (i.e., merely considering the temporal distances), and thus require involving the actual timestamps of check-ins.

Motivated by this observation, we propose REPLAY, a general RNN based architecture learning to capture the varying temporal regularity of human mobility for location prediction. Specifically, REPLAY is designed to seamlessly incor-

¹Note that user check-ins on LBSNs are mostly for social sharing purposes, where check-ins at entertainment-related POIs are much more than those at home-related POIs during the nighttime [Yang *et al.*, 2020b].

porate smoothed timestamp embeddings with learnable bandwidths into the flashback mechanism. More precisely, for each check-in in a check-in sequence, we first transform its time to an hour-in-week timestamp t_n , where $1 \leq n \leq 168$ (one of the 168 hours in a week) and then generate a smoothed timestamp embedding using Gaussian weighted averaging with a timestamp-specific learnable bandwidth σ_n (controlling the width of the Gaussian weighting function centered at the timestamp n). Afterward, we concatenated the smoothed timestamp embedding with the corresponding POI embedding, which is then fed into an RNN with the flashback mechanism, where the spatiotemporal distances in sparse trajectories are used to search for the informative past hidden states. Finally, we combine the hidden state output by the RNN, a user embedding, and a smoothed timestamp embedding generated from a query time to make predictions on future POIs. *The timestamp-specific learnable bandwidths here can automatically learn to adapt to the temporal regularities of different strengths across different timestamps.* Intuitively, a smaller σ_n leads to a peaky Gaussian, which implies a stronger regularity at timestamp n , as the smoothed timestamp embedding relies mostly on the embedding of t_n itself and less on the information from its neighboring timestamps for prediction. This is also evidenced by our experiments later; the learnt bandwidths for the timestamps in the daytime are indeed 7.5% smaller on average than those in the nighttime, which well corresponds to our observations in Figure 1. Our contributions are summarized as follows:

- We revisit the existing sequence models for location prediction, and identify their limitation in capturing the time-varying temporal regularities of human mobility.
- We propose REPLAY, a general RNN architecture capturing the time-varying temporal regularities via smoothed timestamp embeddings using Gaussian weighted averaging with timestamp-specific learnable bandwidths, which can flexibly adapt to the temporal regularities of different strengths across different timestamps.
- We conduct a thorough evaluation using two real-world LBSN datasets. Results show that our REPLAY outperforms a sizable collection of state-of-the-art location prediction methods, with 7.7%-10.9% improvement over the best-performing baselines. Moreover, the learnt bandwidths reveal interesting temporal regularity patterns: 1) morning mobility shows a stronger regularity compared to other time periods, which is consistent on both weekdays and weekends; 2) weekend mobility is less regular than weekdays in general, while the weekend afternoon sometimes shows the weakest regularity.

2 Related Work

Location prediction is one key task of mobility modeling, which predicts a user’s future location based on her historical mobility traces. Traditional methods mainly focus on various mobility features including historical visit counts [Noulas *et al.*, 2012b; Gao *et al.*, 2012], activity preferences [Ye *et al.*, 2013; Yang *et al.*, 2015], social influences [Cho *et al.*, 2011; Sadilek *et al.*, 2012], or automatically-learned features (embedding) [Xie *et al.*, 2016; Feng *et al.*, 2017; Qian *et al.*, 2019;

Yang *et al.*, 2019]. However, these techniques have limited capability of capturing the sequential patterns of user mobility, which have been shown as an important predictor for location prediction [Liu *et al.*, 2016].

To model the sequential patterns of user mobility, early methods often leverage Markov Chains to estimate a transition matrix encoding the probability of visiting a POI conditioned on past visits. For example, for location prediction/recommendation problems, transition matrices are built with factorized personalized Markov Chains with spatial constraints [Cheng *et al.*, 2013; Feng *et al.*, 2015; Zhang *et al.*, 2014a]. However, these methods have intrinsic limitations in capturing the long-term dependencies of visited locations in user mobility traces.

To capture the long-term dependencies, deep learning sequential models (e.g., RNN, LSTM, GRU, and Attention Neural Networks) have been widely used in location prediction tasks. To handle real-world mobility traces that are often sparse and incomplete, spatiotemporal contexts are often considered. A widely adopted approach is to add the spatiotemporal distances between successive check-ins as additional inputs to the RNN units. For example, the spatial distances between successively checked POIs are fed as additional inputs to RNNs [Cui *et al.*, 2019]; STRNN [Liu *et al.*, 2016] designs RNN transition matrices parameterized by the spatiotemporal distances between successive check-ins; HST-LSTM [Kong and Wu, 2018] extends existing gates in LSTMs to allow the spatiotemporal distance as an additional input; STGN [Zhao *et al.*, 2019] incorporates additional gates controlled by the spatiotemporal distances to LSTMs; NeuNext [Zhao *et al.*, 2020] extend STGN via POI context prediction to help next POI recommendation tasks. STAN [Luo *et al.*, 2021] uses spatiotemporal attention networks to capture the dependencies between non-adjacent check-ins; GeoSAN [Lian *et al.*, 2020] uses hierarchical gridding of GPS locations for spatial discretization and uses self-attention layers for matching. Despite the improved performance of these methods, recent studies have shown that considering the spatiotemporal distances between successive check-ins cannot fully capture the temporal periodicity and spatial regularity of human mobility patterns [Yang *et al.*, 2020a], and proposed a flashback mechanism to explicitly use the high-order spatiotemporal distances to search past hidden states with high predictive power (i.e., historical hidden states that share similar spatiotemporal contexts to the current one). For example, Flashback [Yang *et al.*, 2020a] aggregates past hidden states with high predictive power using a context-aware weighting mechanism; BiGRU [Cao *et al.*, 2021] designs a bi-directional GRU with the flashback mechanism; BSDA [Li *et al.*, 2021a] designs a bi-direction speculation method for location prediction, combining flashback with an additional RNN which models POIs’ appeal to users; Bi-STAN [Wu *et al.*, 2022] extends flashback mechanism for missing check-in imputation; RTPM [Liu *et al.*, 2022] combines flashback with real-time user preference models for real-time location recommendation. In addition, on top of the sequence models, researchers also resort to graph-based models to help the location prediction performance, where the graph-based models can easily integrate additional information beyond

trajectory data (e.g., category or user social relationship), such as graph-enhanced attention networks [Li *et al.*, 2021b; Wang *et al.*, 2022b; Wang *et al.*, 2022a], graph-enhanced flashback networks [Rao *et al.*, 2022], and hierarchical multi-task graph recurrent networks [Lim *et al.*, 2022]. However, all of these existing methods overlook the time-varying temporal regularities of user mobility (as evidenced in Figure 1), which motivates us to design REPLAY as presented below.

3 REPLAY

To capture the time-varying temporal regularities of human mobility, we design REPLAY to seamlessly incorporate smoothed timestamp embeddings with learnable bandwidths into the flashback mechanism. Figure 2 shows the overview of our REPLAY. Given a user’s mobility trace denoted as a POI sequence $\{\dots, p_{i-2}, p_{i-1}, p_i, \dots\}$ and its corresponding check-in time $\{\dots, t_{i-2}, t_{i-1}, t_i, \dots\}$, where i denote the order of check-in in the mobility trace, our objective is to predict a future POI p_{i+1} that a user will probably visit at a query time t_{i+1} . To this end, REPLAY first generates a smoothed timestamp embedding for each check-in time in the sequence, and then concatenates it with the corresponding POI embedding which are then fed into an RNN with the flashback mechanism. Finally, we combine the hidden state output by the RNN, a user embedding, and a smoothed timestamp embedding generated from the query time to make predictions on future POIs. We present each component in detail below.

3.1 Smoothed Timestamp Embeddings

To flexibly capture the time-varying temporal regularities of human mobility, REPLAY designs a smoothed timestamp embedding method, which first transforms check-in time into hour-in-week timestamps, and then generates smoothed timestamp embeddings using Gaussian weighted averaging with learnable bandwidths, where cyclical timestamps are considered in the Gaussian kernel.

Hour-in-Week Timestamp Transformation. For i -th check-in in the input mobility trace, we first transform its check-in time t_i into an hour-in-week timestamp t_n , where $1 \leq n \leq 168$ (i.e., one of the 168 hours in a week). For example, $t_i = (15:00 \text{ Tue. } 07/11/2023)$ is transformed into $t_n, n = 39$, as t_i is the 39-th hour in a week. We choose to model the temporal regularity at an hour granularity on a weekly scale, as it can capture not only daily patterns but also the difference between weekdays and weekends, which is also suggested by [Yang *et al.*, 2019]. Moreover, we experimentally justify this design choice by comparing with other time granularities and scales (see experiments and Appendix D for more detail).

Gaussian Smoothing with Learnable Bandwidth. For each timestamp, we initialize a learnable embedding vector, denoted as \vec{t}_n , and compute a smoothed timestamp embedding \vec{s}_n using Gaussian weighted averaging with a learnable bandwidth σ_n , flexibly combining the neighboring timestamp embeddings. This design is inspired by kernel regression techniques [Nadaraya, 1964], and we further incorporate timestamp-specific *learnable* bandwidths here to flexibly capture the temporal regularities of different strengths across different timestamps. Specifically, for the input timestamp t_n ,

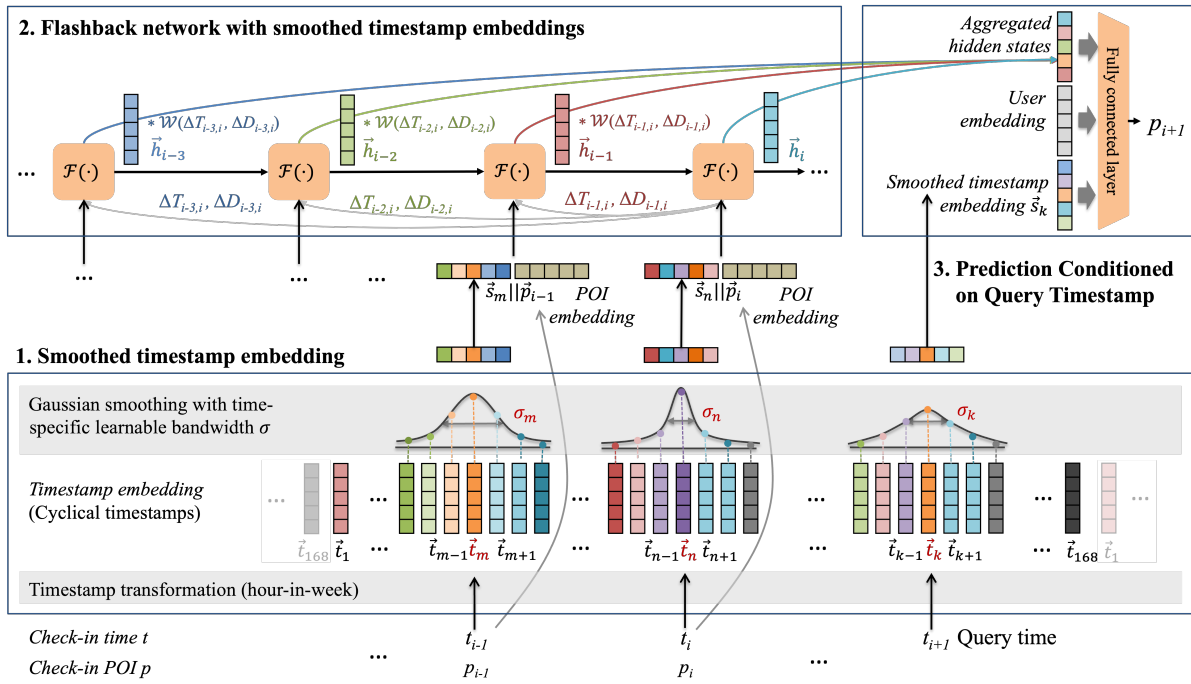


Figure 2: Overview of our proposed REPLAY. It consists of three components: 1) Smoothed timestamp embedding, 2) Flashback network with smoothed timestamp embeddings, and 3) Prediction conditioned on query timestamp.

the Gaussian kernel function is defined as:

$$f_n(l) = \frac{1}{\sigma_n \sqrt{2\pi}} e^{-\frac{\text{dist}(l,n)^2}{2\sigma_n^2}} \quad (1)$$

where $\text{dist}(l, n)$ is a function computing the distance between timestamps l and n . The bandwidth (i.e., standard deviation) σ_n here controls the width of the Gaussian weighting function. A smaller bandwidth σ_n leads to a peaky Gaussian, where the smoothed timestamp embedding of t_n requires less information from its neighboring timestamps; in other words, the location prediction relies mostly on the timestamp embedding of t_n , which implies a stronger regularity at timestamp n . In contrast, a larger bandwidth σ_n leads to a wide Gaussian, where the smoothed timestamp embedding of t_n integrates a significant amount of information from its neighboring timestamps for location prediction, which thus implies a weaker regularity at timestamp n .

Cyclical Timestamps Different from traditional distance metrics in kernel regression, our distance function for hour-in-week timestamps should be carefully designed, as Sunday night 11pm ($l = 168$) and Monday morning 1am ($l = 2$) are only two hours apart, for example. Therefore, we consider cyclical timestamps for the distance computation:

$$\text{dist}(l, n) = \begin{cases} |l - n|, & \text{if } |l - n| < 84 \\ 168 - |l - n|, & \text{otherwise} \end{cases} \quad (2)$$

Afterward, we compute the smoothed timestamp embedding \vec{s}_n as a weighted average of all timestamp embeddings:

$$\vec{s}_n = \frac{\sum_l f_n(l) \cdot \vec{t}_l}{\sum_l f_n(l)} \quad (3)$$

3.2 Flashback with Smoothed Timestamp Embeddings

Flashback Mechanism After obtaining the smoothed timestamp embedding, we feed it together with the corresponding POI embedding to RNN units with the flashback mechanism. Specifically, the flashback mechanism [Yang *et al.*, 2020a] leverages the spatiotemporal context to search past hidden states with high predictive power. It computes the weighted average of the historical hidden states $h_j, j < i$, with a weight $\mathcal{W}(\Delta T_{i,j}, \Delta D_{i,j})$ as an aggregated hidden state for location prediction. This weight is parameterized by the temporal and spatial distances ($\Delta T_{i,j}$ and $\Delta D_{i,j}$, respectively) between check-in (p_i, t_i) and (p_j, t_j), which is defined as follows:

$$\mathcal{W}(\Delta T_{i,j}, \Delta D_{i,j}) = \text{hvc}(2\pi\Delta T_{i,j}) e^{-\alpha\Delta T_{i,j}} e^{-\beta\Delta D_{i,j}} \quad (4)$$

where $\text{hvc}(x) = \frac{1+\cos(x)}{2}$ is the Haversine function capturing the daily periodicity (note that $T_{i,j}$ is measured in days here). The two exponential terms model the temporal and spatial decay of past hidden states, respectively, following the intuition that the hidden states of older and farther check-ins have less predictive power in general; α and β are tunable parameters for decay rates. Please refer to [Yang *et al.*, 2020a] for more details.

Adding Smoothed Timestamp as Input Different from the original Flashback network [Yang *et al.*, 2020a] that only takes POI embeddings as inputs of RNN units, REPLAY concatenates the POI embedding together with the corresponding smoothed timestamp embedding as inputs of the RNN units, i.e., $\vec{h}_i = \mathcal{F}([\vec{p}_i; \vec{s}_n], \vec{h}_{i-1})$, as shown in Figure 2. The objective here is to capture the correlation between a check-in's POI and timestamp. Such a correlation can effectively help the location prediction performance. For example,

working-related POIs are usually checked by users in the daytime. Moreover, our smoothed timestamp embeddings here can *flexibly* capture this correlation by integrating information from neighboring timestamps, where the amount of the information is controlled by the bandwidth σ . Subsequently, the learnable σ can automatically adapt to time-varying temporal regularities; for example, a timestamp with a high mobility regularity will intuitively yield a smaller value of the bandwidth σ , as it relies less on the information from its neighboring timestamps for prediction.

3.3 Prediction Conditioned on Query Timestamp

To predict a future location, we feed the aggregated hidden state with a user embedding and a smoothed timestamp embedding of a query timestamp, to a fully connected layer to output a probability distribution of all POIs.

The design choice of prediction conditioned on timestamp is motivated by the fact that over a sparse user mobility trace, the time intervals between successive check-ins significantly vary. Subsequently, to predict the next check-in in the sequence, the predicted next POI should vary across different “query” time. Therefore, REPLAY is designed to make predictions conditioned on a query time. The same or similar settings exist in the literature by using a query timestamp (same as ours) [Gao *et al.*, 2012; Yang *et al.*, 2019; Li *et al.*, 2021a], a query time interval (to predict the location of a user after a given time period) [Figueiredo *et al.*, 2016; Zhao *et al.*, 2019; Zhao *et al.*, 2020; Feng *et al.*, 2018], or a fixed query time threshold (to predict the location of a user within a forthcoming period of time) [Feng *et al.*, 2015; Zhang *et al.*, 2014a; Feng *et al.*, 2018].

Note that an alternative setting is to make predictions on the next POI without considering the query time [Liu *et al.*, 2016; Yang *et al.*, 2020a; Rao *et al.*, 2022]. We do not advocate for this setting in this paper as it always makes the same prediction for all future time given an input mobility trace, which is less reasonable in real-world scenarios.

3.4 Discussions

In this section, we discuss how REPLAY captures the time-varying temporal regularities by comparing the utility of time interval and (smoothed) timestamps.

Time interval captures the temporal regularity of human mobility over sparse trajectories. The flashback mechanism leverages the spatiotemporal context to search the historical hidden states for location prediction, where the historical hidden states temporally close to the periodicity peaks of returning probability (as shown in Figure 1) are usually more informative for location prediction. For example, Figure 3 shows that using time interval ($\Delta T \approx 1$ day), we can quickly find similar temporal context in sparse trajectories and retrieves the corresponding hidden state for prediction.

Smoothed Timestamps further captures the temporal variation (uncertainty) of the temporal regularities. Specifically, we reveal in this paper that the degree of such uncertainty (or the strength of the temporal regularities) varies across time. Subsequently, the smoothed timestamp embeddings are used to accommodate such variations. Instead of directly using a specific timestamp embedding, we smooth it with

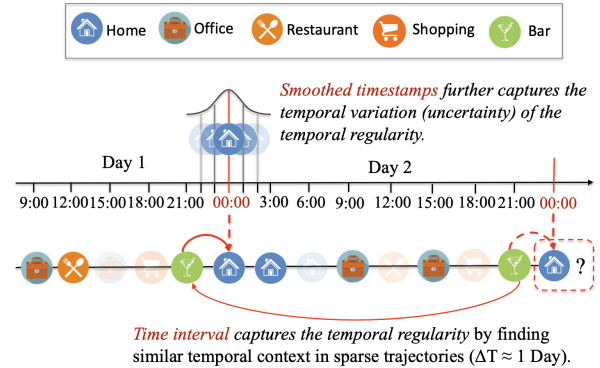


Figure 3: A toy example showing how REPLAY models the time-varying temporal regularities of human mobility.

the neighboring timestamps as shown in Figure 3, where the timestamp-specific learnable bandwidths can automatically adapt to the temporal regularities of different strengths across different timestamps.

Model Training. Please refer to Appendix A for more details about the model training.

4 Experiments

4.1 Experiment Setup

Dataset. We adopt two widely used check-in datasets collected from two LBSNs: **Gowalla** [Cho *et al.*, 2011] and **Foursquare** [Yang *et al.*, 2020b]. Table 2 shows the dataset statistics. Each mobility trace is chronologically split into 80% for training and 20% for testing. Note that as the user mobility regularity depends on local time, we transform the original UTC time of each check-in to a local time according to the time zone of the check-in GPS coordinates.

Baselines. We compare REPLAY against a sizable collection of 18 state-of-the-art techniques from five categories: *User Preference-based Methods* **WRMF** [Hu *et al.*, 2008] and **BPR** [Rendle *et al.*, 2009]; *Feature-based methods* **Most Frequent Time (MFT)** [Gao *et al.*, 2012] and **LBSN2Vec** [Yang *et al.*, 2019]; *Markov-Chain-based Methods* **FPMC** [Rendle *et al.*, 2010], **PRME** [Feng *et al.*, 2015], and **TribeFlow** [Figueiredo *et al.*, 2016]; *Basic RNNs*: **RNN** [Zhang *et al.*, 2014b], **LSTM** (Long Short-Term Memory) [Hochreiter and Schmidhuber, 1997] and **GRU** (Gated Recurrent Unit) [Cho *et al.*, 2014]; *Spatiotemporal Sequence Models* **STRNN** [Liu *et al.*, 2016], **DeepMove** [Feng *et al.*, 2018], **STGN** [Zhao *et al.*, 2019], **STGCN** [Zhao *et al.*, 2019], **STAN** [Luo *et al.*, 2021], **GetNext** [Yang *et al.*, 2022], **Flashback** [Yang *et al.*, 2020a], and **Graph-Flashback** [Rao *et al.*, 2022]. The details about these baselines and their hyperparameter setting can be found in Appendix B.

Evaluation Metrics. We report two widely used metrics for location prediction: average Accuracy@N (Acc@N), where $N = 1, 5, 10$, and Mean Reciprocal Rank (MRR). Please refer to Appendix C for more details about experiment settings.

4.2 Location Prediction Performance

Table 1 shows the location prediction performance of different methods. First, we observe that REPLAY achieves

Table 1: Location prediction performance comparison, where the best-performing ones are highlighted. [†]Methods make predictions using query time information as a query timestamp (MFT, LBSN2Vec, and REPLAY), as a query time interval (TribeFlow, DeepMove, STGN, STGCN, STAN), or as a query time threshold (PRME). Note that DeepMove predicts locations in a fixed future time slot, implicitly implying a fixed query time interval. [◊]Experiments of GetNext are conducted on 15000 randomly sampled users on Foursquare, due to its poor efficiency where it takes more than 24 hours per epoch on the whole Foursquare datasets. The top two best-performing results are denoted in bold and underlined, respectively.

Method		Gowalla				Foursquare			
		Acc@1	Acc@5	Acc@10	MRR	Acc@1	Acc@5	Acc@10	MRR
User Preference based Methods	WRMF	0.0112	0.0260	0.0367	0.0178	0.0278	0.0619	0.0821	0.0427
	BPR	0.0131	0.0363	0.0539	0.0235	0.0315	0.0828	0.1143	0.0538
Feature-based Methods	MFT [†]	0.0525	0.0948	0.1052	0.0717	0.1945	0.2692	0.2788	0.2285
	LBSN2Vec [†]	0.0864	0.1186	0.1390	0.1032	0.2190	0.3955	0.4621	0.2781
Markov-Chain based Methods	FPMC	0.0479	0.1668	0.2411	0.1126	0.0753	0.2384	0.3348	0.1578
	PRME [†]	0.0740	0.2146	0.2899	0.1504	0.0982	0.3167	0.4064	0.2040
	TribeFlow [†]	0.0256	0.0723	0.1143	0.0583	0.0297	0.0832	0.1239	0.0645
Basic RNNs	RNN	0.0881	0.2140	0.2717	0.1507	0.1824	0.4334	0.5237	0.2984
	LSTM	0.0621	0.1637	0.2182	0.1144	0.1144	0.2949	0.3761	0.2018
	GRU	0.0528	0.1416	0.1915	0.0993	0.0606	0.1797	0.2574	0.1245
Spatiotemporal Sequence Models	STRNN	0.0900	0.2120	0.2730	0.1508	0.2290	0.4310	0.5050	0.3248
	DeepMove [†]	0.0625	0.1304	0.1594	0.0982	0.2400	0.4319	0.4742	0.3270
	STGN [†]	0.0624	0.1586	0.2104	0.1125	0.2094	0.4734	0.5470	0.3283
	STGCN [†]	0.0546	0.1440	0.1932	0.1017	0.1878	0.4502	0.5329	0.3062
	STAN [†]	0.0891	0.2096	0.2763	0.1523	0.2265	0.4515	0.5310	0.3420
	GETNext [◊]	0.0912	0.2003	0.2487	0.1484	0.1862	0.4702	0.5763	0.3153
	Flashback	0.1158	0.2754	0.3479	0.1925	0.2496	0.5399	0.6236	0.3805
	Graph-Flashback	<u>0.1512</u>	<u>0.3425</u>	0.4256	<u>0.2422</u>	<u>0.2805</u>	<u>0.5757</u>	<u>0.6514</u>	<u>0.4136</u>
REPLAY [†]	0.1866	0.3476	0.4124	0.2635	0.3529	0.5953	0.6648	0.4638	

Table 2: Statistics of the datasets

Dataset	Gowalla	Foursquare
#Users	52,979	46,065
#POIs	121,851	69,005
#Checkins	3,300,986	9,450,342
Collection period	02/2009-10/2010	04/2012-01/2014

the best performance in most cases, yielding 7.7% and 10.9% improvement over the best-performing baselines on Gowalla and Foursquare, respectively. Moreover, REPLAY significantly outperforms the best baselines in Acc@1 (by 23.4% and 25.8% on Gowalla and Foursquare, respectively). The only exception is on Acc@10 where Graph-Flashback achieves slightly better performance than REPLAY; note that beyond user mobility trajectories, Graph-Flashback further uses user social relationships as input.

We also highlight in Table 1 the nine methods that make predictions using query time information in different formats (e.g., a query timestamp, a query time interval, or a query time threshold). However, we did not observe a consistent improvement of these methods over others that make predictions without using query time information. This is due to the fact that the prediction performance of these baseline methods is dominated by their distinct model structures, rather than the benefit of adding query time information.

Finally, we also conduct a systematic ablation study of REPLAY in Appendix D to verify the usefulness of both our smoothed timestamp embeddings (with 20.6% and 7.5% improvement on Gowalla and Foursquare, respectively) and the query time (with 18.0% and 11.1% improvement on Gowalla and Foursquare, respectively) in location prediction.

4.3 Different Time Granularities and Scales

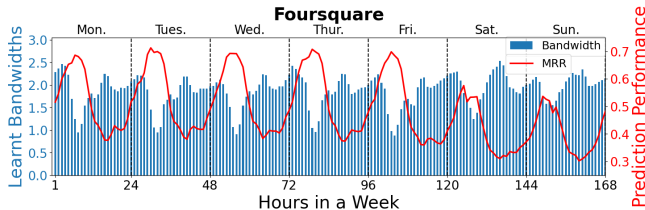
We study the impact of different time granularities (minute or hour) and time scales (day, weekday&weekend or week) in our smoothed timestamp embeddings. Note that for the time scale weekday&weekend, we define two sets of daily cyclical timestamps for weekday and weekend, respectively; the timestamp distance in each set is computed independently. Table 3 shows the different settings and their results.

First, we observe that the week scale consistently outperforms the day scale by 2.89% and 0.74% (on the hour granularity) on Gowalla and Foursquare, respectively. Because the former can capture the different temporal regularities across different days in a week, while the latter cannot. Moreover, compared to the weekday&weekend scale that captures the different regularities on weekdays and weekends, the week scale still achieves better performance (with 1.43% and 0.4% improvement on Gowalla and Foursquare, respectively, under the hour granularity). Because the week scale can further capture the regularity differences between different weekdays (also between different days on the weekend).

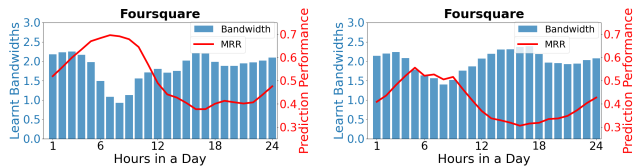
Second, we observe that the hour granularity is generally better than the minute granularity, as the minute granularity is often over-specific to model the temporal regularity of user mobility. One exception is on the week scale on Foursquare where we observe comparable results; however, in this case, the minute granularity shows significantly worse runtime performance (more than twice the training time as shown in Table 3) than the hour granularity, as it needs to learn much more embeddings for minute-in-week timestamps (10,080 in total) than for hour-in-week timestamps (168 in total). Moreover, we also conducted experiments on multi-granularity combining both hour-in-day and day-in-week timestamp em-

Table 3: Impact of different time granularities and scales on location prediction performance

Scale	Granularity	Number of Timestamps	Gowalla					Foursquare				
			Acc@1	Acc@5	Acc@10	MRR	Time per epoch	Acc@1	Acc@5	Acc@10	MRR	Time per epoch
Day	Minute	1440	0.1278	0.2918	0.3610	0.2060	41.35s	0.2801	0.5723	0.6468	0.4121	122.14s
	Hour	24	0.1777	0.3411	0.4063	0.2555	39.35s	0.3483	0.5927	0.6622	0.4601	101.85s
Weekday&Weekend	Minute	2880	0.1804	0.3423	0.4090	0.2577	44.98s	0.3530	0.5938	0.6631	0.4633	142.74s
	Hour	48	0.1821	0.3442	0.4097	0.2594	37.69s	0.3505	0.5941	0.6632	0.4618	102.33s
Week	Minute	10080	0.1756	0.3276	0.3891	0.2485	72.41s	0.3532	0.5940	0.6638	0.4636	264.00s
	Hour	168	0.1866	0.3476	0.4124	0.2635	44.20s	0.3529	0.5953	0.6648	0.4638	103.49s



(a) Hours in week



(b) Hours on weekdays

(c) Hours on weekends

Figure 4: The learnt bandwidths and the corresponding performance across different timestamps on Foursquare.

beddings in Appendix D; the results show 3.4% and 0.6% improvement of our REPLAY over this multi-granularity setting, on Gowalla and Foursquare, respectively. Therefore, we use hour-in-week timestamps in REPLAY.

4.4 Revealing the Time-Varying Temporal Regularities

We reveal the time-vary temporal regularities of user mobility using the learnt bandwidths from REPLAY. Figure 5(a) shows the values of the learnt bandwidths for the 168 hour-in-week timestamps and the corresponding location prediction performance in MRR for each timestamp on Foursquare (similar results on Gowalla as shown in Appendix E).

First, we observe a clear daily pattern, where the bandwidths in the morning have smaller values compared to other time periods; this implies a stronger temporal regularity of the morning mobility (often working-related activities), as the smoothed timestamp embeddings require less information from the neighboring timestamps for location prediction. In contrast, the learnt bandwidths in the nighttime often have larger values, implying a weaker temporal regularity in the nighttime (often entertainment-related activities¹), as the smoothed timestamp embeddings require more information from the neighboring timestamps for location prediction. Moreover, we further compare the bandwidths between weekdays and weekends, by plotting the average bandwidth for each hour on weekdays and on weekends in Figure 5(b) and 5(c), respectively. We observe that despite the similarity of having smaller bandwidths in the morning, the bandwidths

Table 4: Location prediction performance and the corresponding average bandwidth $\bar{\sigma}$ in different time periods.

Prediction time period	Gowalla		Foursquare	
	MRR	$\bar{\sigma}$	MRR	$\bar{\sigma}$
Daytime(6:00-18:00)	0.2767	0.85	0.4856	1.76
Nighttime(18:00-6:00)	0.2362	0.88	0.4302	2.00
Weekday	0.2922	0.82	0.4841	1.84
Weekend	0.1898	0.98	0.3758	2.00

on weekends have larger values than on weekdays, which implies that weekend activities are less regular than weekdays. We find that the weekend afternoon shows the weakest regularity evidenced by the largest bandwidth.

Second, we also observe a clear daily pattern in location prediction performance, which, interestingly, shows an *inverse* trend compared to the bandwidths. This is due to the fact that the weaker regularity of user mobility at a certain timestamp (in the nighttime or on weekends, for example) makes it harder for location prediction; subsequently, the learnt bandwidth has a larger value, as the query timestamp is less confident for location prediction and thus resorts more to its neighboring timestamps for prediction.

Finally, we quantitatively verify our motivating example where the strength of the temporal regularities varies across typical time periods (daytime/nighttime and weekday/weekend). Table 4 shows the average MRR and learnt bandwidths in these periods. We see the daytime prediction performance is 15.0% higher (7.5% lower bandwidth) than the nighttime, while the weekday prediction performance is 41.4% higher (11.9% lower bandwidth) than the weekend.

5 Conclusion

In this paper, we propose REPLAY, a general RNN architecture capturing the time-varying temporal regularities of user mobility for location prediction. It seamlessly incorporates smoothed timestamp embeddings with learnable bandwidths into a flashback mechanism. The timestamp-specific learnable bandwidths can automatically learn to adapt to the temporal regularities of different strengths across different timestamps. We conduct a thorough evaluation using two real-world LBSN datasets. Results show that REPLAY outperforms a sizable collection of state-of-the-art location prediction methods, with 7.7%-10.9% improvement over best-performing baselines, and the learnt bandwidths reveal interesting patterns of the time-varying temporal regularities.

In future work, we plan to study the temporal regularities varying across different user groups and POI categories.

References

- [Cao *et al.*, 2021] Yu Cao, Ang Li, Jinglei Lou, Mingkai Chen, Xuguang Zhang, and Bin Kang. An attention-based bidirectional gated recurrent unit network for location prediction. In *2021 13th International Conference on Wireless Communications and Signal Processing (WCSP)*, pages 1–5. IEEE, 2021.
- [Cheng *et al.*, 2013] Chen Cheng, Haiqin Yang, Michael R Lyu, and Irwin King. Where you like to go next: Successive point-of-interest recommendation. In *IJCAI*, 2013.
- [Cho *et al.*, 2011] Eunjoon Cho, Seth A Myers, and Jure Leskovec. Friendship and mobility: user movement in location-based social networks. In *KDD*, pages 1082–1090. ACM, 2011.
- [Cho *et al.*, 2014] Kyunghyun Cho, Bart Van Merriënboer, Caglar Gulcehre, Dzmitry Bahdanau, Fethi Bougares, Holger Schwenk, and Yoshua Bengio. Learning phrase representations using rnn encoder-decoder for statistical machine translation. *arXiv:1406.1078*, 2014.
- [Cui *et al.*, 2019] Qiang Cui, Yuyuan Tang, Shu Wu, and Liang Wang. Distance2pre: Personalized spatial preference for next point-of-interest prediction. In *PAKDD*, pages 289–301. Springer, 2019.
- [Deng *et al.*, 2023] Bangchao Deng, Dingqi Yang, Bingqing Qu, Benjamin Fankhauser, and Philippe Cudre-Mauroux. Robust location prediction over sparse spatiotemporal trajectory data: Flashback to the right moment! *ACM Transactions on Intelligent Systems and Technology*, 14(5):1–24, 2023.
- [Feng *et al.*, 2015] Shanshan Feng, Xutao Li, Yifeng Zeng, Gao Cong, Yeow Meng Chee, and Quan Yuan. Personalized ranking metric embedding for next new poi recommendation. In *IJCAI*, 2015.
- [Feng *et al.*, 2017] Shanshan Feng, Gao Cong, Bo An, and Yeow Meng Chee. Poi2vec: Geographical latent representation for predicting future visitors. In *AAAI*, 2017.
- [Feng *et al.*, 2018] Jie Feng, Yong Li, Chao Zhang, Funing Sun, Fanchao Meng, Ang Guo, and Depeng Jin. Deepmove: Predicting human mobility with attentional recurrent networks. In *WWW*, pages 1459–1468, 2018.
- [Figueiredo *et al.*, 2016] Flavio Figueiredo, Bruno Ribeiro, Jussara M Almeida, and Christos Faloutsos. Tribeflow: Mining & predicting user trajectories. In *WWW*, pages 695–706, 2016.
- [Gao *et al.*, 2012] Huiji Gao, Jiliang Tang, and Huan Liu. Exploring social-historical ties on location-based social networks. In *ICWSM*, 2012.
- [Gonzalez *et al.*, 2008] Marta C Gonzalez, Cesar A Hidalgo, and Albert-Laszlo Barabasi. Understanding individual human mobility patterns. *Nature*, 453(7196):779, 2008.
- [Hochreiter and Schmidhuber, 1997] Sepp Hochreiter and Jürgen Schmidhuber. Long short-term memory. *Neural computation*, 9(8):1735–1780, 1997.
- [Hu *et al.*, 2008] Yifan Hu, Yehuda Koren, and Chris Volinsky. Collaborative filtering for implicit feedback datasets. In *ICDM*, pages 263–272. Ieee, 2008.
- [Kong and Wu, 2018] Dejiang Kong and Fei Wu. Hst-ilstm: A hierarchical spatial-temporal long-short term memory network for location prediction. In *IJCAI*, pages 2341–2347, 2018.
- [Li *et al.*, 2021a] Xixi Li, Ruimin Hu, Zheng Wang, and Toshihiko Yamasaki. Location predicts you: Location prediction via bi-direction speculation and dual-level association. In *IJCAI*, pages 529–536, 2021.
- [Li *et al.*, 2021b] Yang Li, Tong Chen, Yadan Luo, Hongzhi Yin, and Zi Huang. Discovering collaborative signals for next poi recommendation with iterative seq2graph augmentation. *arXiv preprint arXiv:2106.15814*, 2021.
- [Lian *et al.*, 2015] Defu Lian, Xing Xie, Vincent W Zheng, Nicholas Jing Yuan, Fuzheng Zhang, and Enhong Chen. Ccpr: A collaborative exploration and periodically returning model for location prediction. *TIST*, 6(1):8, 2015.
- [Lian *et al.*, 2020] Defu Lian, Yongji Wu, Yong Ge, Xing Xie, and Enhong Chen. Geography-aware sequential location recommendation. In *Proceedings of the 26th ACM SIGKDD international conference on knowledge discovery & data mining*, pages 2009–2019, 2020.
- [Lim *et al.*, 2022] Nicholas Lim, Bryan Hooi, See-Kiong Ng, Yong Liang Goh, Renrong Weng, and Rui Tan. Hierarchical multi-task graph recurrent network for next poi recommendation. 2022.
- [Liu *et al.*, 2016] Qiang Liu, Shu Wu, Liang Wang, and Tieniu Tan. Predicting the next location: A recurrent model with spatial and temporal contexts. In *AAAI*, 2016.
- [Liu *et al.*, 2022] Xin Liu, Yongjian Yang, Yuanbo Xu, Funing Yang, Qiuyang Huang, and Hong Wang. Real-time poi recommendation via modeling long-and short-term user preferences. *Neurocomputing*, 467:454–464, 2022.
- [Luo *et al.*, 2021] Yingtao Luo, Qiang Liu, and Zhaocheng Liu. Stan: Spatio-temporal attention network for next location recommendation. In *Proceedings of the Web Conference 2021*, pages 2177–2185, 2021.
- [Mikolov *et al.*, 2010] Tomáš Mikolov, Martin Karafiát, Lukáš Burget, Jan Černocký, and Sanjeev Khudanpur. Recurrent neural network based language model. In *INTER-SPEECH*, 2010.
- [Nadaraya, 1964] Elizbar A Nadaraya. On estimating regression. *Theory of Probability & Its Applications*, 9(1):141–142, 1964.
- [Neil *et al.*, 2016] Daniel Neil, Michael Pfeiffer, and Shih-Chii Liu. Phased lstm: Accelerating recurrent network training for long or event-based sequences. In *NIPS*, pages 3882–3890, 2016.
- [Noulas *et al.*, 2012a] Anastasios Noulas, Salvatore Scellato, Renaud Lambiotte, Massimiliano Pontil, and Cecilia Mascolo. A tale of many cities: universal patterns in human urban mobility. *PloS one*, 7(5):e37027, 2012.

- [Noulas *et al.*, 2012b] Anastasios Noulas, Salvatore Scellato, Neal Lathia, and Cecilia Mascolo. Mining user mobility features for next place prediction in location-based services. In *ICDM*, pages 1038–1043. IEEE, 2012.
- [Qian *et al.*, 2019] Tiejun Qian, Bei Liu, Quoc Viet Hung Nguyen, and Hongzhi Yin. Spatiotemporal representation learning for translation-based poi recommendation. *TOIS*, 37(2):18, 2019.
- [Rao *et al.*, 2022] Xuan Rao, Lisi Chen, Yong Liu, Shuo Shang, Bin Yao, and Peng Han. Graph-flashback network for next location recommendation. In *Proceedings of the 28th ACM SIGKDD Conference on Knowledge Discovery and Data Mining*, pages 1463–1471, 2022.
- [Rendle *et al.*, 2009] Steffen Rendle, Christoph Freudenthaler, Zeno Gantner, and Lars Schmidt-Thieme. Bpr: Bayesian personalized ranking from implicit feedback. In *UAI*, pages 452–461. AUAI Press, 2009.
- [Rendle *et al.*, 2010] Steffen Rendle, Christoph Freudenthaler, and Lars Schmidt-Thieme. Factorizing personalized markov chains for next-basket recommendation. In *WWW*, pages 811–820. ACM, 2010.
- [Sadilek *et al.*, 2012] Adam Sadilek, Henry Kautz, and Jeffrey P Bigham. Finding your friends and following them to where you are. In *WSDM*, pages 723–732. ACM, 2012.
- [Wang *et al.*, 2022a] Zhaobo Wang, Yanmin Zhu, Haobing Liu, and Chunyang Wang. Learning graph-based disentangled representations for next poi recommendation. In *Proceedings of the 45th International ACM SIGIR Conference on Research and Development in Information Retrieval*, pages 1154–1163, 2022.
- [Wang *et al.*, 2022b] Zhaobo Wang, Yanmin Zhu, Qiaomei Zhang, Haobing Liu, Chunyang Wang, and Tong Liu. Graph-enhanced spatial-temporal network for next poi recommendation. *ACM Transactions on Knowledge Discovery from Data (TKDD)*, 16(6):1–21, 2022.
- [Wu *et al.*, 2022] Junhang Wu, Ruimin Hu, Dengshi Li, Lingfei Ren, Wenyi Hu, and Yilin Xiao. Where have you been: Dual spatiotemporal-aware user mobility modeling for missing check-in poi identification. *Information Processing & Management*, 59(5):103030, 2022.
- [Xie *et al.*, 2016] Min Xie, Hongzhi Yin, Hao Wang, Fanjiang Xu, Weitong Chen, and Sen Wang. Learning graph-based poi embedding for location-based recommendation. In *CIKM*, pages 15–24. ACM, 2016.
- [Yang *et al.*, 2015] Dingqi Yang, Daqing Zhang, Vincent W Zheng, and Zhiyong Yu. Modeling user activity preference by leveraging user spatial temporal characteristics in lbsns. *TSMC*, 45(1):129–142, 2015.
- [Yang *et al.*, 2019] Dingqi Yang, Bingqing Qu, Jie Yang, and Philippe Cudre-Mauroux. Revisiting user mobility and social relationships in lbsns: a hypergraph embedding approach. In *WWW*, pages 2147–2157. ACM, 2019.
- [Yang *et al.*, 2020a] Dingqi Yang, Benjamin Fankhauser, Paolo Rosso, and Philippe Cudré-Mauroux. Location prediction over sparse user mobility traces using rnns: Flashback in hidden states! In *IJCAI*, pages 2184–2190, 2020.
- [Yang *et al.*, 2020b] Dingqi Yang, Bingqing Qu, and Philippe Cudre-Mauroux. Location-centric social media analytics: Challenges and opportunities for smart cities. *IEEE Intelligent Systems*, 36(5):3–10, 2020.
- [Yang *et al.*, 2022] Song Yang, Jiamou Liu, and Kaiqi Zhao. Getnext: trajectory flow map enhanced transformer for next poi recommendation. In *Proceedings of the 45th International ACM SIGIR Conference on research and development in information retrieval*, pages 1144–1153, 2022.
- [Ye *et al.*, 2013] Jihang Ye, Zhe Zhu, and Hong Cheng. What’s your next move: User activity prediction in location-based social networks. In *SDM*, pages 171–179. SIAM, 2013.
- [Ye *et al.*, 2023] Ziming Ye, Xiao Zhang, Xu Chen, Hui Xiong, and Dongxiao Yu. Adaptive clustering based personalized federated learning framework for next poi recommendation with location noise. *IEEE Transactions on Knowledge and Data Engineering*, 2023.
- [Zhang *et al.*, 2014a] Jia-Dong Zhang, Chi-Yin Chow, and Yanhua Li. Lore: Exploiting sequential influence for location recommendations. In *Proceedings of the 22nd ACM SIGSPATIAL International Conference on Advances in Geographic Information Systems*, pages 103–112, 2014.
- [Zhang *et al.*, 2014b] Yuyu Zhang, Hanjun Dai, Chang Xu, Jun Feng, Taifeng Wang, Jiang Bian, Bin Wang, and Tie-Yan Liu. Sequential click prediction for sponsored search with recurrent neural networks. In *AAAI*, 2014.
- [Zhao *et al.*, 2019] Pengpeng Zhao, Haifeng Zhu, Yanchi Liu, Jiajie Xu, Zhixu Li, Fuzhen Zhuang, Victor S Sheng, and Xiaofang Zhou. Where to go next: A spatio-temporal gated network for next poi recommendation. In *AAAI*, volume 33, pages 5877–5884, 2019.
- [Zhao *et al.*, 2020] Pengpeng Zhao, Anjing Luo, Yanchi Liu, Fuzhen Zhuang, Jiajie Xu, Zhixu Li, Victor S Sheng, and Xiaofang Zhou. Where to go next: A spatio-temporal gated network for next poi recommendation. *IEEE Transactions on Knowledge and Data Engineering*, 2020.
- [Zhu *et al.*, 2017] Yu Zhu, Hao Li, Yikang Liao, Beidou Wang, Ziyu Guan, Haifeng Liu, and Deng Cai. What to do next: Modeling user behaviors by time-lstm. In *IJCAI*, pages 3602–3608, 2017.

A The details of our Model Training

The training process of REPLAY follows the traditional backpropagation-through-time training process of recurrent neural networks. For each prediction, we compute the cross-entropy loss between the probability distribution of POIs output by REPLAY and the ground truth POIs, which are minimized using Adam optimizer. The loss function is defined as follows:

$$\mathcal{L} = -\frac{1}{U} \sum_{j=1}^U \frac{1}{N_j - 1} \sum_{i=1}^{N_j-1} y_{i+1,j} \log(p(\hat{y}_{i+1,j} | \mathcal{H}_i, s_k, u_j))$$

Table 5: Ablation study on REPLAY

Method	Gowalla				Foursquare			
	Acc@1	Acc@5	Acc@10	MRR	Acc@1	Acc@5	Acc@10	MRR
Flashback (RNN)	0.1158	0.2754	0.3479	0.1925	0.2496	0.5399	0.6236	0.3805
Flashback (LSTM)	0.1024	0.2575	0.3317	0.1778	0.2398	0.5169	0.6014	0.3654
Flashback (GRU)	0.0979	0.2526	0.3267	0.1731	0.2375	0.5154	0.6003	0.3631
REPLAY-noSTE (RNN)	0.1362	0.3099	0.3845	0.2185	0.3055	0.5690	0.6415	0.4251
REPLAY-noSTE (LSTM)	0.1263	0.2980	0.3724	0.2079	0.3002	0.5663	0.6396	0.4209
REPLAY-noSTE (GRU)	0.1356	0.3099	0.3856	0.2183	0.2993	0.5634	0.6360	0.4192
REPLAY-noQT (RNN)	0.1397	0.3169	0.3924	0.2237	0.2817	0.5744	0.6489	0.4139
REPLAY-noQT (LSTM)	0.1343	0.3123	0.3873	0.2187	0.2739	0.5620	0.6360	0.4043
REPLAY-noQT (GRU)	0.1319	0.3105	0.3866	0.2168	0.2716	0.5623	0.6376	0.4029
REPLAY-MultiG (RNN)	0.1856	0.3357	0.3942	0.2570	0.3501	0.5894	0.6578	0.4598
REPLAY-MultiG (LSTM)	0.1808	0.3314	0.3904	0.2527	0.3440	0.5816	0.6493	0.4529
REPLAY-MultiG (GRU)	0.1798	0.3310	0.3897	0.2520	0.3426	0.5797	0.6477	0.4513
REPLAY-FixedB(RNN)	0.1861	0.3419	0.4024	0.2601	0.3513	0.5899	0.6575	0.4607
REPLAY-FixedB (LSTM)	0.1837	0.3411	0.4032	0.2587	0.3438	0.5817	0.6498	0.4528
REPLAY-FixedB (GRU)	0.1817	0.3374	0.3991	0.2558	0.3418	0.5807	0.6487	0.4512
REPLAY (RNN)	0.1866	0.3476	0.4124	0.2635	0.3529	0.5953	0.6648	0.4638
REPLAY (LSTM)	0.1848	0.3467	0.4100	0.2618	0.3448	0.5850	0.6544	0.4549
REPLAY (GRU)	0.1826	0.3449	0.4091	0.2597	0.3430	0.5831	0.6524	0.4530

where U is the number of users; N_j is the sequence length of j -th user; $y_{i+1,j}$ is the one-hot vector of ground truth POI for $(i+1)$ -th check-in of j -th user. $p(\hat{y}_{i+1,j}|\mathcal{H}_i, s_k, u_j)$ is the predicted probability distribution given the current aggregated hidden state \mathcal{H}_i , smoothed query timestamp s_k (transformed from time t_{i+1}), and user embedding u_j .

B The details of baselines

The details of baselines and the hyperparameters as follow:

- *User Preference-based Methods*. **WRMF** is a matrix factorization based recommendation technique designed explicitly for implicit feedback such as historical user behavior, where users do not explicitly express their preference; it fits well our check-in datasets that contain historical user presence at POIs. **BPR** is a ranking-based recommendation technique for implicit feedback, which learns user preferences by minimizing a pairwise ranking loss; it uses a bootstrap sampling technique to learn from both positive feedback and non-observed feedback to alleviate data sparsity issue. We use the default parameter settings of LibRec² for these two methods.
- *Feature-based methods*: Most Frequent Time (**MFT**) ranks a POI according to a user’s historical check-in count at a POI and at a specific time slot in the training dataset; we define the timeslot as 24 hours in a typical day as suggested by paper. **LBSN2Vec** is an automatic feature learning technique designed specifically for check-in data; it learns user, time and POI feature vectors from an LBSN hypergraph, and ranks a POI according to its similarities with user and time in the feature space for location prediction tasks; we set the number of negative samples, random walk window size, and the mobility data ratio to $\{10, 10, 1\}$ in our experiments.
- *Markov-Chain-based Methods*: **FPMC** estimates a personalized transition matrix of POIs in user mobility trajectories using matrix factorization techniques. We set the number of negative samples and the dimension of factorization to $\{10, 32\}$. **PRME** extends FPMC to location prediction problems by further considering spatial constraints, and learns user and POI embeddings to capture the personalized POI transition patterns. We set the threshold, component weight, and hidden state size to $\{360, 0.2, 20\}$. **TribeFlow** learns a mixture model to capture the semi-Markov transition probability matrix over latent environments for predicting user trajectories. We set the number of cores, number of transitions, number of iterations, and the number of batches to $\{20, 0.3, 2000, 20\}$, and use ECCDF-based kernel introduced in paper.
- *Basic RNNs*: **RNN** is a vanilla Recurrent Neural Network architecture, capturing sequential patterns from user mobility trajectories for location prediction. **LSTM** (Long Short-Term Memory) is capable of learning from both short- and long-term dependency in sequences using a memory cell controlled by three multiplicative gates including an input gate, an output gate and a forget gate. **GRU** (Gated Recurrent Unit) captures long-term dependency by controlling information flow with an update gate and a reset gate. We set the hidden state size to 10 for all three RNN architectures and all the datasets.
- *Spatiotemporal Sequence Models*: **DeepMove** adds an attention mechanism to GRU for location prediction over sparse mobility trajectories. We set the size of all embeddings and the hidden state size to $\{50, 10\}$, and use average history mode and LSTM as suggested by paper. **STRNN** uses customized transition matrices parameterized by the spatiotemporal distances between check-ins within a time window in RNNs. **STGN** adds additional gates controlled by the spatiotemporal distances between successive check-ins to LSTM. **STGCN** is an extension of STGN with coupled input and forget gates for improved efficiency. We set the hidden state size to 10 for all the datasets. **STAN** designs a spatiotemporal attention network

²<https://github.com/guoguibing/librec>

Table 6: Coefficient of variation in MRR over different RNN architectures (RNN, LSTM, GRU). A large value indicates a large variation in the performance over different RNNs.

Method	Gowalla	Foursquare
Basic RNNs	21.73%	41.84%
Flashback	5.59%	2.55%
REPLAY-noSTE	2.82%	0.71%
REPLAY-noQT	1.64%	1.47%
REPLAY-MultiG	1.06%	0.99%
REPLAY-FixedB	0.84%	1.12%
REPLAY	0.73%	1.26%

capturing interactions between non-adjacent locations and non-consecutive check-ins using spatiotemporal contexts. We set the embedding size, the maximum length for trajectory sequence, and the number of negative samples to $\{50, 100, 10\}$, respectively. **GetNext** exploits the user flow trajectory graph and time-aware category context embedding for next location prediction; for a fair comparison, we do not use category information by assigning the same category to all POIs. We set the embedding size of POIs and users, the numbers of three GCN layers’ channels, the embedding size of the transformer encoder to $\{128, 32, 64, 128, 1024\}$, respectively. **Flashback** aggregates past hidden states with high predictive power using a context-aware weighting mechanism; **Graph-Flashback** incorporates a User-POI knowledge graph into the Flashback framework, where the social relationships between users are also used. We set α and β as suggested by Flashback in Graph-Flashback and Flashback.

C Experiment Settings

We developed our model using the PyTorch framework and conducted experiments on the following hardware platform (CPU: Intel(R) Xeon(R) Gold 5320, GPU: NVIDIA GeForce RTX 3090). We empirically set the dimension of hidden states and all (POI, timestamp, and user) embedding sizes as 10, and the temporal decay factor α and spatial decay factor β following the suggested settings in Flashback.

D Ablation Study

We conduct an ablation study on our proposed method REPLAY, considering the following variants.

- **REPLAY-noSTE** is a variant of REPLAY without the Smoothed Timestamp Embeddings (noSTE). It is also equivalent to Flashback by adding the query time interval for prediction.
- **REPLAY-noQT** is a variant of REPLAY making predictions without using the Query Time (noQT). It is also equivalent to Flashback integrated with the smoothed timestamp embeddings.
- **REPLAY-MultiG** is a variant of REPLAY combining multi-granularity (hour-in-day and day-in-week) timestamp embeddings.
- **REPLAY-FixedB** is a variant of REPLAY with a universal fixed non-learnable bandwidth.

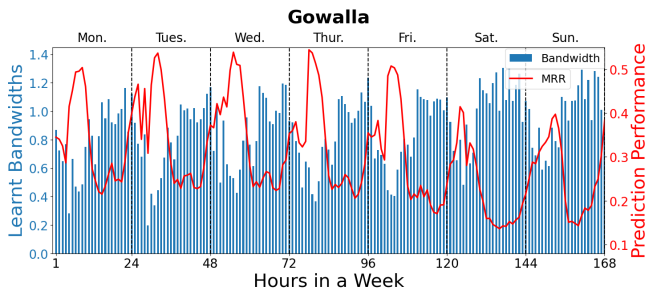
- **Flashback** can also be considered as a variant of REPLAY without the smoothed timestamp embeddings or query time.

For each method, we instantiate it with the three common RNN architectures (vanilla RNN, LSTM, or GRU). Table 5 shows the results. First, we observe that our smoothed timestamp embeddings can significantly improve the location prediction performance by flexibly capturing the time-varying temporal regularities of human mobility. The improvement is evidenced by the superiority of REPLAY over REPLAY-noSTE (20.6% and 7.5% improvement on Gowalla and Foursquare, respectively). Second, we observe that the prediction conditioned on query time can also improve the location prediction performance as the query time intuitively provides additional information for location prediction problems, which results in the improvements of REPLAY over REPLAY-noQT (18.0% and 11.1% improvement on Gowalla and Foursquare, respectively). Finally, compared to Flashback, REPLAY integrating smoothed timestamp embeddings and making predictions conditioned on query time yields a significant improvement of 43.9% and 21.8% on Gowalla and Foursquare, respectively.

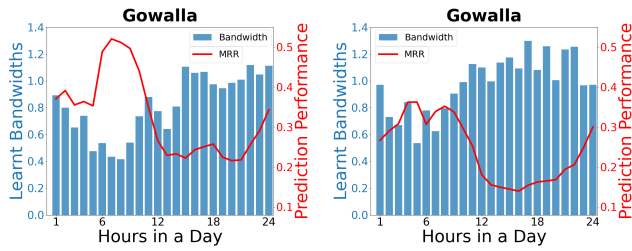
To further explore the impact of different granularities and the timestamp-specific learnable bandwidths, we conducted experiments on two variants of REPLAY, named REPLAY-MultiG (Multi-Granularity) and REPLAY-FixedB (Fixed Bandwidth). From Table 5, we observe that REPLAY consistently yields better performance (3.4% and 0.6% improvement on Gowalla and Foursquare, respectively) over REPLAY-MultiG, which further validates our design choice of hour-in-week timestamps. Besides, we observe that REPLAY with timestamp-specific learnable bandwidths achieves consistently better performance (1.5% and 0.6% improvement on Gowalla and Foursquare, respectively) over REPLAY-FixedB, which shows the necessity of using timestamp-specific learnable bandwidths in location prediction.

In addition, we also investigate the performance of using different RNN architectures (vanilla RNN, LSTM, or GRU). We observe that the vanilla RNN yields the best performance in general, while LSTM and GRU show comparable results. This is probably due to the fact that the flashback mechanism is able to effectively find useful historical hidden states using spatiotemporal contexts for location prediction, which indeed weakens the utility of retaining long-term memory by LSTM or GRU.

Interestingly, we find that REPLAY is more robust than Flashback against different RNNs. Specifically, we measure the robustness using a coefficient of variation, defined as the ratio of the standard deviation to the mean of a variable. We compute the coefficient of variation on the performance using different RNNs, and compare the results from different methods. Table 6 shows the results. We observe that compared to basic RNNs, Flashback can effectively reduce the coefficient of variation from 21.73% and 41.84% to 5.59% and 2.55% on Gowalla and Foursquare, respectively. More importantly, REPLAY can further reduce the coefficient of variation to 0.73% and 1.26% on Gowalla and Foursquare, respectively. In other words, integrating smoothed timestamp embeddings



(a) Hours in week



(b) Hours on weekdays

(c) Hours on weekends

Figure 5: The learnt bandwidths and the corresponding location prediction across different timestamps on Gowalla.

and making predictions conditioned on query time can make our model more robust against different RNNs.

E The Time-Varying Temporal Regularities on Gowalla

As shown in Figure 5, similar to the Foursquare dataset, we observe a clear daily pattern, where the bandwidths in the morning have smaller values in general compared to other time periods and the bandwidths on weekends have larger values than on weekdays. Despite the daily pattern of the learnt bandwidths, we also observe a clear daily pattern (an *inverse* trend compared to the bandwidths) in location prediction performance.